

High-sensitivity silicon carbide optical MEMS accelerometer based on wavelength modulation system

HUANG Kun^{1,2}, CHENG Lin², QU Shuai², LIU Yuxiang², CUI Jianguo², HE Xinhui², HU Qin²

(1. Upgrading Office of Modern College of Humanities and Sciences, Shanxi Normal University, Linfen 041000, China;

2. State Key Laboratory of Dynamic Testing Technology, North University of China, Taiyuan 030051, China)

Abstract: This paper reports a high-frequency silicon carbide (SiC) sensor that relies on dual-mode wavelength modulation and its application to optical microelectromechanical systems (MEMS). Based on the properties of as well as SiC and the characteristics of dual-mode analysis, an optical MEMS sensor suitable for a high-frequency field is designed. In addition, the finite element analysis (FEA) method with ANSYS and the rigorous coupled wave analysis (RCWA) method are used. A comparison with other high-frequency sensors shows that the proposed sensor displays advantages with respect to properties such as a wide measurement range, high sensitivity, and almost zero cross-axis sensitivity. The proposed optical sensor provides an optical sensitivity ($\Delta\lambda/\Delta a$) of 2.247 7, a mechanical sensitivity of 0.155 nm/g and an almost zero cross-axis sensitivity in the entire operation measurement range. The first resonance frequency is 40.035 kHz, the linear measurement range is ± 129.03 g, the sensitivity of the sensing system ($\Delta\lambda/\Delta a$) is 0.348 4 nm/g, and the working bandwidth is 35 kHz.

Key words: microelectromechanical system (MEMS); wavelength modulation; optical accelerometer

0 Introduction

In recent decades, integrated inertial micro electro mechanical system (MEMS) sensors have experienced significant development, with a wide range of applications from the automotive industry^[1-2], aerospace^[3], consumer electronics^[4], and biomedical sciences^[5] to earthquake monitoring^[6]. In addition, accelerometers have a wide range of applications in the field of non-destructive testing (NDT), including bearing detection^[7-8], condition monitoring systems of wind energy industry^[9-10], tool condition monitoring^[11-12], identification of bridge dynamic parameters^[13], and non-intrusive-fault detection technique for thermal reciprocating engines^[14-15]. Displacement measurements include piezoresistive^[16-17], piezoelectric^[18-19], capacitive^[20-23], tunnel current^[24], and optical^[25-32] measurements, among others. Each sensing technique has its own advantages and disadvantages.

Piezoelectric and piezoresistive sensors are very sensitive to changes in humidity and temperature,

therefore, their application areas are limited in many ways. However, due to its low manufacturing price and simple manufacturing method, the capacitive approach is the most popular technique in accelerometer industry even though there are several drawbacks, such as the curling effect^[21], parasitic capacitance, high sensitivity to electromagnetic interference (EMI) in the low-frequency range, and small capacitance changes caused by external accelerations. The basic sensing principle is a system that senses the displacement of a proof mass. The displacement of the mass block is used to cause a change in the output voltage or current and thus ultimately to calculate the acceleration. The optical sensing mechanism avoids the above shortcomings owing to its unique performance. Compared with other sensing technologies^[16-24], optical sensors offer an intrinsic immunity to EMI, a higher thermal stability, and a wider operational bandwidth. In optical MEMS sensors, the principle of the sensing system is based on the modulation of light wave properties, such as the intensity, phase and wave length. Wavelength modulation^[33-35] has the

Received date: 2022-12-28

Foundation items: Graduate Education Reform Project (No. 18001215); Scientific and Technological Innovation Project (No. 18004438)

Corresponding author: CHENG Lin (kiki.cheng@nuc.edu.cn)

advantage of resisting light source fluctuations. To date, photonic crystals have intensely attracted the focus of researchers.

Silicon is a common material in optical sensors because of its excellent properties. Although silicon material has good optical properties, its application in the high-frequency field is limited due to its low Young's modulus (~ 169 GPa).

Therefore, a high sensitivity and a wide measurement range cannot be achieved simultaneously. High-frequency sensors are usually limited by the contradiction between the frequency band and the sensitivity and cannot achieve both a high sensitivity and a wide measurement range simultaneously on high-frequency devices^[26-28]. From a material point of view, common materials have been used for decades in the electronic industry and have been studied for optical MEMS sensors. Therefore, the study of new materials is limited in this field. When using new materials with unique properties, the original habits are followed.

Silicon carbide (SiC) is a material with great potential. A comparison with silicon shows that SiC displays a high Young's modulus and high density. The Young's modulus of SiC reaches 490 GPa, and the density reaches 3.100 kg/m^3 . One of the important characteristics of a MEMS accelerometer is the first resonance, which depends on the mechanical system and relies on the stiffness and the mechanical resonator mass. Therefore, SiC has a great advantage with regard to its mechanical structure design. Sufficient linearity of the accelerometer can be achieved by a simple mechanical structure, which also reduces the manufacturing difficulty of the process. In addition, in our research, we found that SiC leads to an interesting phenomenon through wavelength modulation. Based on this dual-mode modulation, a high-sensitivity optical modulation system is proposed to be integrated into a SiC optical accelerometer^[33]. Here, we propose a high-frequency SiC sensor that relies on dual-mode wavelength modulation. In the field of high-frequency sensors, the proposed sensor provides a wide measurement range, high sensitivity and a wide working bandwidth.

The rest of this paper can be summarized as follows: The whole operation and design principle of the proposed accelerometer is presented in section 1; The discussion and analysis of the optical sensing system are carried out in section 2; The mechanical

modeling and analysis are discussed in section 3; In section 4, a comparison between the proposed sensor and some recently developed high-frequency sensors is presented; And the final conclusions and perspectives are given in section 5.

1 Design and principle

The proposed optical accelerometer relies on the wave length modulation and optical properties of SiC. A schematic of the proposed sensor is illustrated in Fig. 1.

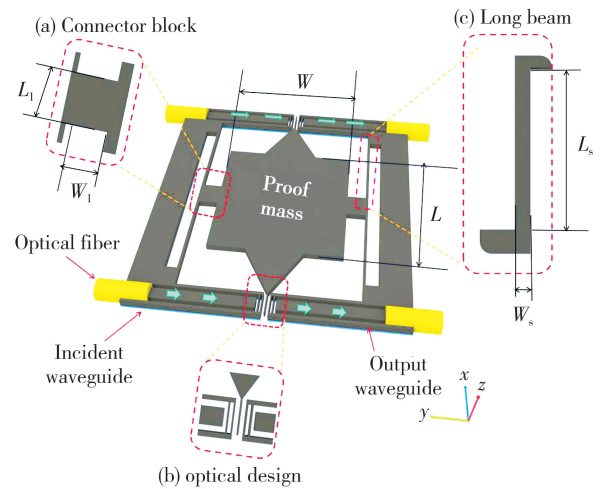


Fig. 1 3D structure of proposed SiC optical MEMS accelerometer sensor

By using a typical lighting emitting diode (LED) light source, a photodetector, five SiC fingers and an integrated optical waveguide, the optical sensing system based on MEMS accelerometer sensor is designed. The operation principle of the accelerometer is summarized as follows. Two symmetrical one-dimensional photonic crystal systems^[18] are located in the center of the waveguide, and each system is composed of five SiC fingers spaced at regular intervals. First, the broadband light source is coupled to the SiC waveguide through an optical fiber. Then, the signal passes through the photonic crystal and is captured by the photodetector. The photodetector converts these optical signals into electrical signals through photoelectric conversion. When external acceleration is applied, the movable finger attached to the proof mass moves laterally along the sensing direction (Y) inside the photonic crystal, which causes the wavelengths of the output defect modes to change. The magnitude and direction of acceleration can then be calculated by the relative change between the two selected output defect modes.

2 Analysis and discussion of optical system

Since the parameters of an accelerometer greatly affect the structure of the optical sensing system, researchers have always believed it is important to determine the optical simulation model well. In this study, an optical simulation model was established according to rigorous coupled wave analysis (RCWA)^[27]. As shown in Fig. 2, the optical system consists of five staggered SiC layers spaced by air. Therefore, some defects are introduced in the optical crystal structure. The moveable finger attached to the proof mass, which we call the optical finger, is the middle finger of five layers. When an external acceleration is applied, the movement of the optical finger breaks the original periodic structure, which leads to transmitted optical modes moving in the photonic band gap of the photonic crystal.

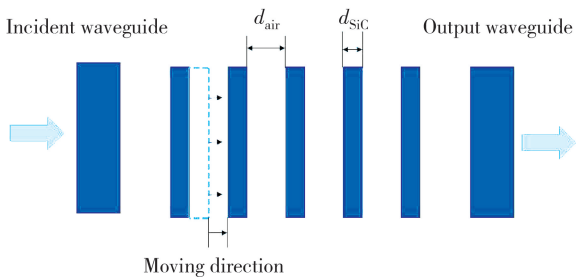


Fig. 2 Schematic of photonic sensing system

In general, the larger the mechanical displacement, the wider the photonic band gap. There is a difference between the carborundum layer width (d_{SiC}) and air layer width (d_{air}) to reflect an extreme range of wavelength gaps. For that, one-quarter of the wavelength width is determined as the width of the SiC and air regions in the system. In addition, the $1.55 \mu\text{m}$ communication band is commonly used in optical sensing technology, so the primary wavelength is selected as $\lambda = 1.55 \mu\text{m}$. In the case where the incoming light is perpendicular, λ , the dielectric index of refraction (n) and the width of the layer (d) obey

$$\lambda/4 = nd, \quad (1)$$

where $\lambda = 1.55 \mu\text{m}$ and $n = 2.61$, $d_{\text{SiC}} = 148.5 \text{ nm}$ and $d_{\text{air}} = 387.5 \text{ nm}$, respectively; and d_{SiC} and d_{air} are the thicknesses of silicon layer and air layer, respectively.

This paper presents a method for analyzing the dual-mode wavelength modulation of the accelerometer. The advantage of this is that it can

achieve higher optical sensitivity than when using a single peak. Further discussion follows below.

The optical reflectivity reaches the highest value at the central wavelength, and the wavelengths close to the central wavelength have a high reflectivity. Therefore, an optical band gap forms, as mentioned above. The application of the band gap is elaborated in detail according to the following content. In this study, we found that there are two special transmission peaks in the photonic band gap because of the displacement of the moveable finger. This is the key part of our design of the optical system.

The main goal of this part is to determine the relative change in the respective central wavelength of the output transmitted defect modes in terms of the change in the applied acceleration. Fig. 3 shows the transmission curves of the designed optical system. In this study, we take the analytical method of double-defect mode motion^[24]. Specifically, the peak wavelength changes due to different optical finger displacements. When there is a slight shift, the two optical defect modes move in opposite directions simultaneously.

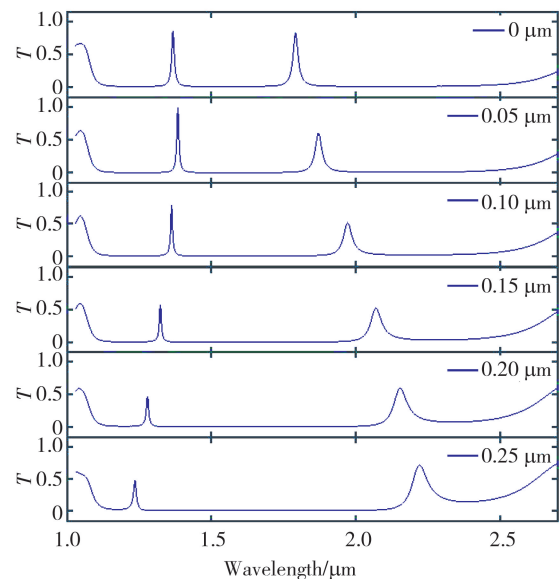


Fig. 3 Transmission curves of carborundum one-dimensional photonic crystal system. Vertical coordinate represents transmissivity and horizontal coordinate represents corresponding wavelength

Since the magnitude and direction can be calculated by the relative changes between two selected output transmitted defect modes, the accelerometer can distinguish between the negative and positive directions. Therefore, the structure is designed such that the movable finger is positioned in the center of the linear response measurement of the structure in

the absence of the applied acceleration. The following is an analysis of the optical linear response.

When the optical finger position changes, the optical crystal presents defects with abnormal periodic changes, and then the corresponding transmission peak appears. In terms of this kind of wavelength modulation, the initial position of the optical finger is located at the side of the measurement range of the one-dimensional optical crystal system. Here, we define the initial position as $\Delta d = 0$.

For high precision, we set 388 locations from $0 \mu\text{m}$ to $0.387 \mu\text{m}$. In terms of the characteristics of Fig. 4, we define the right mode as defect mode 1, which moves toward the direction in which the wavelength increases, and the other mode as defect mode 2 as Δd increases. The top diagrams in Fig. 3 correspond to $\Delta d = 0$ and the following diagrams follow a pattern in which the next diagram is $0.05 \mu\text{m}$ larger than the one before.

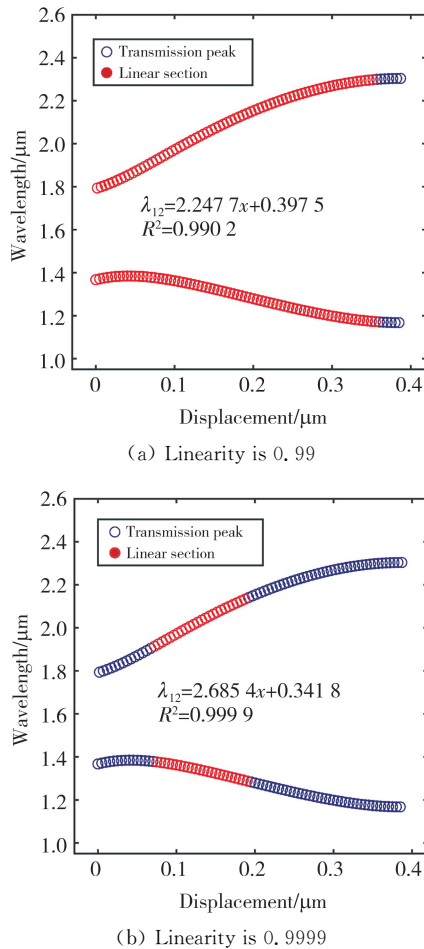


Fig. 4 Wavelength variations of transmission peak versus displacement changes of proof mass. The red part of figure is a linear response. Note that λ_{12} is relative change in wavelength between two peaks, and X is the position of movable finger.

Let us combine Fig. 4 with Fig. 3. The photonic band gap width directly determines the detection range, and they are positively correlated. By fitting the peak wavelength, we found that the transmitted defect mode 1 and mode 2 behave approximately linearly with respect to the relative displacement within limits. Furthermore, the slopes of the two models are negatively correlated, which means that the relative change between the two defect modes is more obvious. Simultaneously, a more detailed analysis is provided for designing a reasonable optical modulation system.

In Fig. 4, “ $\lambda_{12} = 2.2477x + 0.3975$ ” and “ $\lambda_{12} = 2.6854x + 0.3418$ ” (μm) are the linear approximations of the wavelength relative variations of the two peaks as functions of the applied acceleration in the whole measurement range with linearities of 0.99 and 0.9999, respectively. Experimental data show that the proposed detection relies on two consecutive peaks in the spectral response of the actuated photonic crystal. Both peaks are approximately $0.5 \mu\text{m} - 1 \mu\text{m}$ apart. This range can be measured by a wide band spectrometer, or it can be divided into two different bands of spectrometers, and the information can be processed together. In this study, we theoretically analyze the wave band in which the signal exists. Engineering can choose the appropriate detection method according to this.

More detailed results of our experimental system are as follows: the linearity reaches sensitivities of 0.9902 and 2.2477 from $\Delta d = 0 \mu\text{m}$ to $\Delta d = 0.355 \mu\text{m}$, respectively. While greater linearity is required, we can achieve a sensitivity of 2.6854 in the wavelength modulation range from $\Delta d = 0.068 \mu\text{m}$ to $\Delta d = 0.19 \mu\text{m}$ with a linearity of 0.9999. The above indicators and parameters affect the measurement range of the proposed accelerometer. It is obvious that there is always a compromise between the optical modulation range and linearity. In the matter of the specific application field, we typically select reasonable parameters. For a highly sensitive photodetector, we apply a linearity of 0.9999.

Based on the above analysis, our method has a large advantage. In other words, for the same photodetectors, a better device resolution can be provided by the relative modulation of two defect modes. For some materials with low optical sensitivity, “another high sensitivity” is selected.

3 Modeling and analysis of mechanical system

The design of the mechanical structure of the proposed accelerometer directly determines its mechanical properties. In this study, we propose the structure shown in Fig. 1. The proof mass and long

beams are linked by connector blocks. When an external acceleration is applied in the sensing direction (y -axis), the proof mass shifts by a certain displacement, which would result in changes in the optical system.

The related geometrical parameters are illustrated in Table 1 and discussed further.

Table 1 Geometrical parameters of the MEMS accelerometer

Symbol	Parameter	Value
E/GPa	Young's modulus of SiC	490
$\rho/(\text{kg} \cdot \text{m}^{-3})$	Density of SiC	3 100
r	Poisson ratio of SiC	0.142
n_{SiC}	Refractive index of SiC	2.61
$L \times W/(\mu\text{m} \times \mu\text{m})$	Length \times width of proof mass	200 \times 200
$L_s \times W_s/(\mu\text{m} \times \mu\text{m})$	Length \times width of proof beam	250 \times 2
$L_1 \times W_1/(\mu\text{m} \times \mu\text{m})$	Length \times width of proof connector beam	25 \times 15
$T/\mu\text{m}$	Structure thickness	60
$M/\mu\text{g}$	Proof mass	7.44

For further analysis of the dynamic behavior of the proposed accelerometer, it is modeled by a second-order mass damping spring system. In addition, according to the second-order differential equation, the relative displacement y in the direction of compression/tension (sensing-axis, on y -axis) of the second-order differential equation and the relative displacement y of the proof mass by the applied acceleration are illustrated as

$$m \frac{d^2 y}{dt^2} + c \frac{dy}{dt} + ky = ma, \quad (2)$$

where k , c and y are the total spring constant, damping coefficient and relative displacement in the sensing direction, respectively, and m is the effective mass.

In Eq. (2), k is determined by the four mechanical long beams of the proposed accelerometer. Based on the basic beam theory, the spring constants of a fixed beam with length (l), width (w) and thickness (t) along the x -axis, y -axis, and z -axis are given by

$$k_x = \frac{2Et w}{l}, \quad (3)$$

$$k_y = \frac{Et w^3}{l^3}, \quad (4)$$

$$k_z = \frac{Et w^3}{l^3}, \quad (5)$$

where E is Young's modulus (460 GPa for SiC).

In this study, $w = W_s$, $l = L_s/2$, and t is the

structural thickness of the proposed accelerometer, as seen in Fig. 1 and Table 1. Combined with the proposed mechanical design, we can derive $k = 4k_x$. Simultaneously, using $\omega_n = \sqrt{k/M}$, $\delta = c/(2\sqrt{kM})$ and M (proof mass) = 7.44 μg , we have

$$\frac{dy^2}{dt^2} + 2\delta\omega_n \frac{dy}{dt} + \omega_n^2 y = a, \quad (6)$$

where δ is the damping ratio of the system, and ω_n is the radial frequency of the vibration system.

One of the important characteristics is the first resonance that affects the sensor operational bandwidth. For the proposed device, the first resonance frequency (natural frequency) can be approximated as

$$f_r = \frac{\omega_n}{2\pi}. \quad (7)$$

According to the above, we can carry out a theoretical analysis and determine the first resonance frequency to be 40.469 kHz, and the error is 0.08% when compared with the actual result of 40.036 kHz. The theoretical analysis is in good agreement with the practical results (see Fig. 5).

In ordinary optical sensors, the mechanical measurement range usually limits the optical measurement range. However, the unique properties of SiC greatly improve the embarrassing situation. Since SiC has a high Young's modulus, we can reach enough first resonance frequency to extend the band-width. The operational frequency range of the

system has thus been broadened. To further substantiate this, we compare the performance of different materials (carborundum and silicon) with the same geometric parameters and analyze them in principle. A further investigation is described below.

As mentioned above, $\omega_n = \sqrt{k/M}$. To obtain a sufficient operating bandwidth, we need to increase the spring constant k and reduce the effective mass m . For this goal, we can start from two aspects: selecting suitable materials and designing a reasonable geometric structure.

From the material point of view, Young's modulus E is positively correlated with the spring constant k , and the mass density is positively correlated with the mass m . A comparative analysis of silicon and SiC shows that the Young's modulus is 169 GPa and the density is 2 330 kg/m³ for silicon^[26], while the Young's modulus is 490 GPa and the density is 3 100 kg/m³ for SiC. Taking both into consideration, using SiC instead of silicon in the same geometric design, the operational bandwidth of the proposed accelerometer is extended to the square root of two times the original.

From the point of view of geometric parameter design, there is always a compromise with respect to the relationship between different parameters as well

as the fabrication constraints. Among the numerous indicators measured by the accelerometer, the measurement range and sensitivity are contradictory and mutually limited, and the pursuit of increasing one value inevitably leads to decreasing the other.

Because of the use of SiC, not only are the design requirements of high-frequency sensors fully satisfied, but the manufacturing difficulty is also effectively reduced. After a long time of in-depth study and parameter comparison, we found the appropriate geometric parameters in terms of the measurement range, linearity and manufacturing difficulty. The specific data are listed in Table 1.

After determining these important values, we found that the first resonance frequency is 40.035 kHz, and the bandwidth is approximately 35 kHz. If silicon is used instead of SiC, the first resonance frequency is only 27.4 kHz, and the corresponding operating bandwidth is reduced.

The response under different resonance frequencies is an important characteristic of inertial accelerometers. Moreover, the resonant signals seriously affect the detection accuracy, so that the frequency response at different resonances should be analyzed. The first four resonance frequencies are simulated by finite element analysis (FEA).

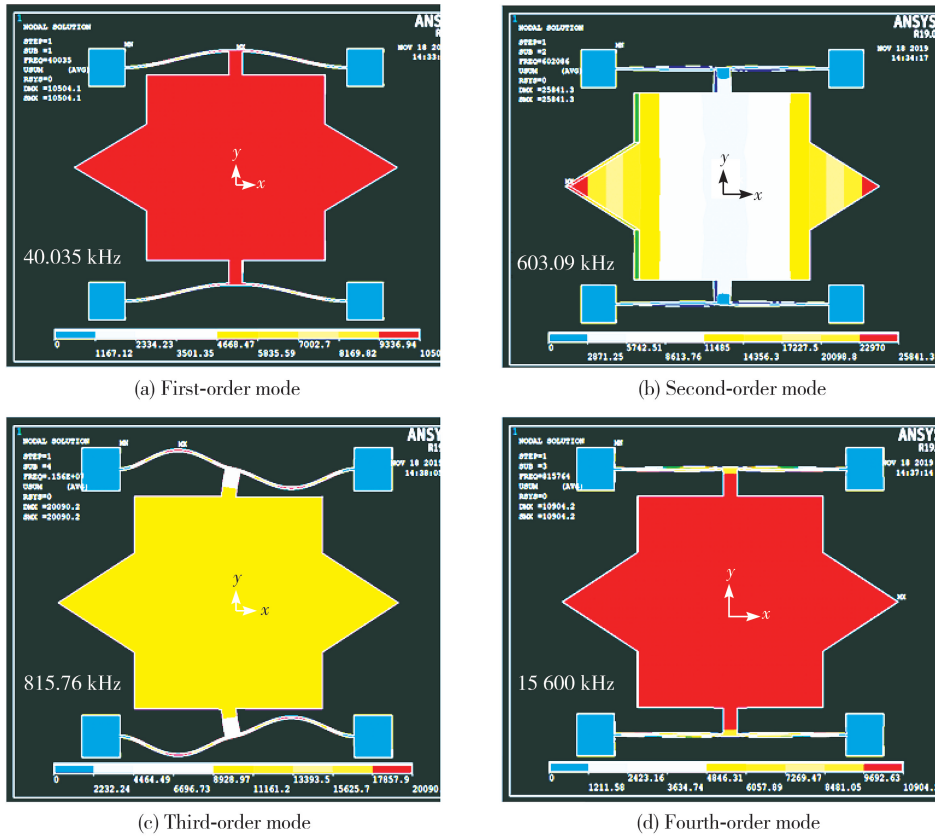


Fig. 5 Modal analysis of proposed MEMS accelerometer

The dynamic behavior of the proposed accelerometer has also been investigated by using ANSYS. The first four vibration modes are shown in Fig. 5. Normally, the first vibration mode is selected as the working mode, and the design requires that the other resonance frequency be large enough to be separated from the first resonance frequency. If this condition is not met, the accelerometer is in an unstable state and is easily broken. For example, the third resonance corresponding to the rotation around the z -axis may damage the accelerometer. The fourth resonance may lead to z -axis displacement of the movable finger.

As shown in Fig. 6, the harmonic response analysis of the accelerometer can be carried out through the modal superposition method. Accordingly, we found that the response is relatively flat from 0 kHz to 35 kHz. Therefore, the operational band-width (0 kHz to 35 kHz) of the proposed accelerometer is lower than the natural frequency (40.035 kHz). However, it is quite a large number compared with that of other reports^[17-19]. After determining these important values, we found that the first resonance frequency of 40.035 kHz has a bandwidth of approximately 35 kHz. If silicon is used instead of carborundum, the first resonance frequency is only 27.4 kHz, and the corresponding operating bandwidth is reduced.

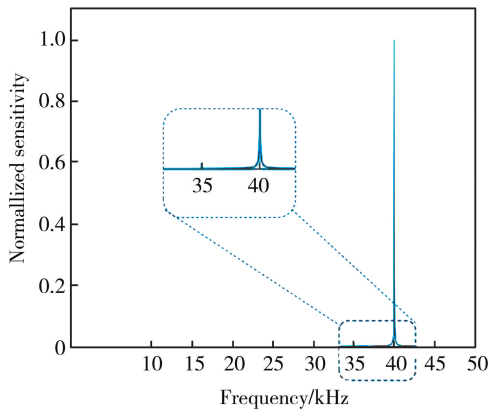


Fig. 6 Harmonic response analysis of proposed accelerometer

Cross-axis sensitivity is an important index to measure the performance of high-frequency sensors. To demonstrate the test results intuitively, linear fits of experimental data are presented in the form of double ordinates in Fig. 7. The cross-axis errors of the accelerometer are extracted as 0.07% and 0.25% for the x -axis and y -axis, respectively. It is obvious that the cross-axis sensitivity of the accelerometer is almost zero.

At the end of this section, we describe the mechanical sensitivity ($\Delta d/\Delta a$), which is related to a key characteristic of an optical system called accelerometer sensitivity ($\Delta\lambda/\Delta a$). As shown in Fig. 7, its slope is its mechanical sensitivity. Further information is described in next section.

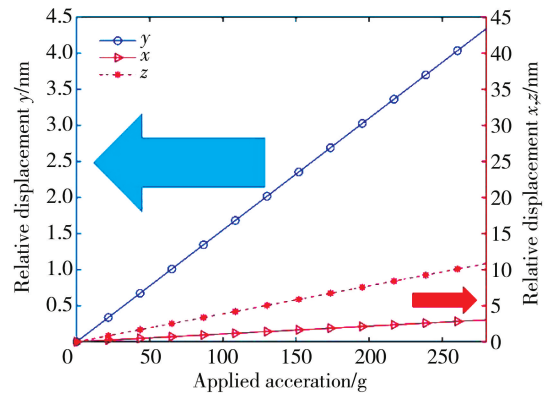


Fig. 7 Mechanical linearity test results of proposed accelerometer along x -axis, y -axis and z -axis, left longitudinal axis corresponds to y -axis, and right longitudinal axis corresponds to x -, z -axes

4 Comparison and discussion

Each performance of the accelerometer is interrelated. The resolution of the proposed accelerometer can be calculated by

$$\delta a = \delta\lambda / S, \tag{8}$$

with

$$S = S_o S_m, \tag{9}$$

where $\delta\lambda$ denotes the minimum resolution of the spectrum analyzer, S denotes the accelerometer sensitivity, S_o denotes the optical system sensitivity, and S_m denotes the mechanical sensitivity. Therefore, in the case of the same spectrometer performance, the higher the accelerometer sensitivity, the lower the resolution of the proposed accelerometer. The performance of the accelerometer is thus better.

Because the application here is a theoretical calculation, the performance of the analysis is based on the current high-precision spectrometer with a 10-pm resolution to discuss the sensitivity and resolution of the accelerometer.

In this section, a comparative review is carried out between the proposed sensor and several recent contributions of high-frequency sensors. The parameters that are used for the comparison are collected in Table 2. Currently, more optical MEMS accelerometers prefer to use silicon and graphene as materials, so we have compared various parameters

with accelerometers made of these two materials.

Table 2 makes it clear that the proposed accelerometer has great advantages. The sensitivity, which depends on optical sensitivity and mechanical sensitivity, is a significant parameter. Due to the method of dual-mode wavelength modulation, a higher optical sensitivity and a wide wavelength modulation range are obtained at the same time. The higher the optical sensitivity, the better the sensor resolution. Moreover, the operational measurement range is the key factor limiting sensor applications. The application field would be wider with a greater operational measurement range. It is worth mentioning that the high Young's modulus of SiC is an excellent advantage. This leads to satisfactory

parameter results for sensors. For example, an almost zero cross-axis sensitivity can be obtained through reasonable design.

In addition, the high Young's modulus also benefits the operation frequency. The proposed sensor has significant advantages compared with the references mentioned. Thus, sensors have great applications in related fields, such as railway industry, earthquake detection, and health monitoring.

There is always a compromise between sensitivity and measurement range. Although a high Young's modulus inevitably leads to low mechanical sensitivity, the final sensitivity is still proper because of the optical sensitivity, as mentioned above.

Table 2 Parameters comparison of proposed sensor and other sensors

Parameter	Proposed sensor	Ref. [17]	Ref. [18]	Ref. [19]
Material	SiC	Graphene	Silicon	Graphene
Footprint of proof mass/ μm	200 \times 200	220 \times 220	220 \times 220	220 \times 220
Sensitivity of sensing system $\Delta\lambda/\Delta a/(\text{nm} \cdot \text{g}^{-1})$	0.348 4	0.211	1.17	0.075 6
Mechanical sensitivity of sensor $\Delta d/\Delta a/(\text{nm} \cdot \text{g}^{-1})$	0.155	0.461	3.18	1.6
Optical sensitivity of sensor $\Delta\lambda/\Delta d$	2.247 7	0.457 2	0.368	0.047 2
Measurement range/g	± 129.03	± 189	± 22	± 156
First resonance frequency/kHz	40.035	23.032	8.908	12.935
Operational bandwidth/kHz	35	8	2	Not reported
Cross-axis sensitivity/%	0.07 (<i>x</i> -axis) 0.25 (<i>y</i> -axis)	almost zero	zero	zero
Resolution ($\Delta\lambda = 10 \text{ pm}$)/mg	28.7	47.37	8.547	132

5 Conclusions

In this paper, a high-frequency optical accelerometer based on wavelength modulation is presented. Detection and analysis of the optical sensing system is accomplished using two-defect mode motion. The performance of the optical sensor system and mechanical parts is analyzed through a FEA simulation. The simulations show that the proposed optical sensor provides an optical sensitivity of 0.348 4 nm/g, a mechanical sensitivity of 0.155 nm/g and almost zero cross-axis sensitivity in the whole operational measurement range, a first resonance frequency of 40.035 kHz, a negligible linear measurement range of $\pm 129.03 \text{ g}$, a sensitivity of the sensing system ($\Delta\lambda/\Delta d$) of 2.247 7 and an operational bandwidth of 35 kHz.

MEMS accelerometers are already being used for bearing sensing and detection^[7-8]. a properly structured MEMS sensor can be integrated onto, or even into, the bearing race. Such integrated solution is expected to improve prognostics capability of the

health status of bearings. Other than that, the combination of vibration analysis by accelerometers and acoustic emission (AE) analysis can improve the sensitivity of wind energy condition detection systems^[9-10]. Also in the field of identification of bridge dynamic parameters, tool condition monitoring and nonintrusive fault detection technique for thermal reciprocating engines^[11-15], a comprehensive solution by enhancing the vibration characteristics and structural parameters of accelerometers is expected to provide better detection and more reliable diagnosis.

However, there are still many restrictions in the wave length modulation accelerometer. Their realization relies on the development of the designed optical system, and there is still much work to be done to make the processing technology leap from a microscale line width to a nanoscale linewidth. In addition, the high-resolution spectrum detection system increases the manufacturing cost of the device. However, the proposed accelerometer has a variety of advantages that make it appealing for

various applications in precision measurement.

The use of deep reactive ion etching (DRIE) can be considered a method to realize MEMS accelerometers with this structure^[37]. However, considering the high chemical stability of SiC, the etch selectivity and masking material are important factors in etching evaluations^[38-39]. The University of California, Berkeley used ALN, which has a selectivity of 16:1, as a SiC masking material to etch SiC, which successfully prevented micro masking defects on the etch surface^[40]. Zhao et al. presented using photo-electro-chemical etching single-crystal wafer to fabricate SiC devices^[41]. A method using ultraviolet light, ultraviolet laser cutting to release cantilever beams of SiC accelerometers and laser ablation to process masses could be acceptable^[42]. Since this article focuses on the theoretical analysis and simulation of the proposed accelerometer, this fabrication may be the subject of a completely different paper. This article does not discuss fabrication in detail.

References

- [1] FLEMING W J. Overview of automotive sensors. *IEEE Sensors Journal*, 2001, 1(4): 296-308.
- [2] ACAR C, SCHOFIELD A R, TRUSOV A A, et al. Environmentally robust MEMES vibratory gyroscope for automotive applications. *IEEE Sensor Journal*, 2009, 9(12): 1895-1906.
- [3] JUDY J W. Microelectromechanical systems (MEMS): Fabrication, design and applications. *Smart Materials and Structures*, 2001, 10(6): 1115-1134.
- [4] BOGUE R. Recent developments in MEMS sensors: A review of applications, markets and technologies. *Sensor Review*, 2013, 33(4): 300-304.
- [5] QUAGLIARELLA L, SASANELLI N, CAVONE G, et al. Biomedical signal analysis by a low-cost accelerometer measurement system//*IEEE Instrumentation and Measurement Technology Conference*, Apr. 24-27, 2006, Sorrento, Italy. New York: IEEE, 2006: 2236-2239.
- [6] TU R, WANG R, GET M, et al. Cost-effective monitoring of ground motion related to earthquakes, landslides, or volcanic activity by joint use of a single frequency GPS and a MEMS accelerometer. *Geophysical Research Letters*, 2013, 40(15): 3825-3829.
- [7] KHMELNITSKY M, BORTMAN J, TURET M, et al. Improved bearing sensing for prognostics: from vibrations to optical fibres. *Insight: Non-Destructive Testing and Condition Monitoring*, 2015, 57(8): 437-441.
- [8] SAFIZADEH M S, GOLMOHAMMADI A. Ball bearing fault detection via multi-sensor data fusion with accelerometer and microphone. *Insight: Non-Destructive Testing and Condition Monitoring*, 2021, 63(3): 168-175.
- [9] RAFAEL S, ROMERO A, GOODFELLOW G, et al. Detection of gearbox failures by combined acoustic emission and vibration sensing in rotating machinery. *Insight: Non-Destructive Testing and Condition Monitoring*, 2014, 56(8): 422-425.
- [10] SOUA S, CEBULSKI L, BRIDGE B, et al. Online monitoring of a power slip-ring on the shaft of a wind power generator. *Insight: Non-Destructive Testing and Condition Monitoring*, 2014, 53(6): 321-329.
- [11] NAKANDHRAKUMAR R S, DINAKARAN D, GOPAL M, et al. A novel normalisation procedure for the sensor positioning problem in vibration monitoring of drilling using artificial neural networks. *Insight: Non-Destructive Testing and Condition Monitoring*, 2016, 58(10): 556-563.
- [12] LAURILA J, LAHDELMA S. Advanced fault diagnosis by means of complex order derivatives. *Insight: Non-Destructive Testing and Condition Monitoring*, 2014, 56(8): 439-442.
- [13] MCGETRICK P J, GONZALEZ A, OBRIEN E J, et al. Theoretical investigation of the use of a moving vehicle to identify bridge dynamic parameters. *Insight: Non-Destructive Testing and Condition Monitoring*, 2009, 51(8): 433-438.
- [14] ALBARBAR A, GU F, BALL A, et al. Internal combustion engine lubricating oil condition monitoring based on vibro-acoustic measurements. *Insight: Non-Destructive Testing and Condition Monitoring*, 2007, 49(12): 715-718.
- [15] BROATCH A, TORMOS B, OLMEDA P, et al. A contribution to the diagnosis of internal combustion engines through rolling block oscillations. *Insight: Non-Destructive Testing and Condition Monitoring*, 2008, 50(11): 637-641.
- [16] ROY A L, SARKAR H, DUTTA A, et al. A high precision SOI MEMS-CMOS ± 4 piezoresistive accelerometer. *Sensors and Actuators A: Physical*, 2014, 210: 77-85.
- [17] XU Y, ZHAO L B, DING J J, et al. Analysis and design of a novel piezoresistive accelerometer with axially stressed self-supporting sensing beams. *Sensors and Actuators A: Physical*, 2016, 247: 1-11.
- [18] LEVINZON F A. Ultra-low-noise seismic piezoelectric accelerometer with integral FET amplifier. *IEEE Sensors Journal*, 2012, 12(6): 2262-2268.
- [19] STADIGADAPA S, MATETI K. Piezoelectric MEMS sensors: state-of-the art and perspectives. *Measurement Science and Technology*, 2009, 20(9): 092001.
- [20] MISTRY K K, SWAMY K B, SEN S, et al. Design of an SOI-MEMS high resolution capacitive type single axis accelerometer. *Microsystem Technologies*, 2010, 16(12): 2057-2066.
- [21] EDALATFAR F, YAGHOOTKAR B, AZIMI S, et al. Development of a micromachined accelerometer for particle acceleration detection. *Sensors and Actuators A:*

- Physical, 2018, 280: 359-367.
- [22] UTZ A, WALK C, STANITZKI A, et al. A high-precision and high-bandwidth MEMS-based capacitive accelerometer. *IEEE Sensors Journal*, 2018, 18(16): 6533-6539.
- [23] HE J, ZHOU W, HU H, et al. Structural designing of a MEMS capacitive accelerometer for low temperature coefficient and high linearity. *Sensors*, 2018, 18(2): 643.
- [24] ROCKSTAD H K, REYNOLDS J K, TANG T K, et al. A miniature, high-sensitivity, electron tunneling accelerometer. *Sensors and Actuators A: Physical*, 1996, 53: 227-231.
- [25] HUANG K, CAO L Q, ZHAI P C, et al. High sensitivity system theoretical research base on waveguide-nano DBRs one dimensional photonic crystal microstructure. *Optics Communications*, 2020, 470: 125392.
- [26] AHMADIAN M, JAFARI K. A graphene-based wide-band MEMS accelerometer sensor dependent on wavelength modulation. *IEEE Sensors Journal*, 2019, 19(15): 6226-6232.
- [27] SHEIKHALEH A, ABEDI K, JAFARI K, et al. A proposal for an optical MEMS accelerometer relied on wavelength modulation with one dimensional photonic crystal. *Journal of Lightwave Technology*, 2016, 34(22): 5244-5249.
- [28] ASGRI S, GRANPAYEH N. Tunable plasmonically induced reflection in graphene-coupled side resonators and its application. *Journal of Nanophotonics*, 2017, 11(2): 026012.
- [29] KRISHNAMOORTHYA U, OLSSON III R H, BOGART G R, et al. In-plane MEMS-based nano-g accelerometer with sub-wavelength optical resonant sensor. *Sensors and Actuators A: Physical*, 2008, 145: 283-290.
- [30] SHEIKHALEH A, ABEDI K, JAFARI K, et al. Micro-optoelectromechanical systems accelerometer based on intensity modulation using a one-dimensional photonic crystal. *Applied Optics*, 2016, 55(32): 8993-8999.
- [31] SHEIKHALEH A, JAFARI K, ABEDI K, et al. Design and analysis of a novel MOEMS gyroscope using an electrostatic comb-drive actuator and an optical sensing system. *IEEE Sensors Journal*, 2018, 19(1): 144-150.
- [32] SAURABH A, MISHRA JITENDRA K, PRIYE V, et al. Highly sensitive MOEMS integrated photonic crystal cavity resonator for nano-mechanical sensing. *Optics Communications*, 2020, 474: 126108.
- [33] HUANG K, NIE Y L, LIU Y X, et al. A proposal for a high-sensitivity optical MEMS accelerometer with double-mode modulation system. *Journal of Lightwave Technology*, 2021, 39: 303-309.
- [34] HUANG K, NIE Y L, YANG J P, et al. A proposal to enhance high-frequency optical MEMS accelerometer sensitivity based on a one-dimensional photonic crystal wavelength modulation System. *IEEE Sensors Journal*, 2020, 20: 14639-14645.
- [35] HUANG K, YU M, CHEN L, et al. A proposal for an optical MEMS accelerometer with high sensitivity based on wavelength modulation system. *Journal of Lightwave Technology*, 2019, 37: 5474-5478.
- [36] MOHARAM M G, GAYLORD T K. Rigorous coupled-wave analysis of metallic surface-relief gratings. *Journal of the Optical Society of America A*, 1986, 3: 1780.
- [37] GHOLAMZADEH R, JAFARI K, CHAROONI M, et al. Design, simulation and fabrication of a MEMS accelerometer by using sequential and pulsed-mode DRIE processes. *Journal of Micromechanics and Microengineering*, 2016, 27(1): 015022.
- [38] MABOUDIAN R, CARRAO C. Advances in silicon carbide science and technology at the micro and nanoscales. *Journal of Vacuum Science & Technology A*, 2013, 31(5): 050805.
- [39] DI G, WIJESUNDARA M B J, CARRARO C, et al. Transformer coupled plasma etching of 3C-SiC films using fluorinated chemistry for micro electro mechanical system applications. *Journal of Vacuum Science & Technology B: Microelectronics and Nanometer Structures Processing, Measurement, and Phenomena*, 2004, 22(2): 513-528.
- [40] SENESKY D G, PISANO A P. Aluminum nitride as a masking material for the plasma etching of silicon carbide structures//*IEEE 23rd International Conference on Micro Electro Mechanical Systems*, Jan. 24-28, 2010, Hong Kong, China. New York: IEEE, 2010: 352-355.
- [41] ZHAO F, LSLAM M M, HUANG C F, et al. Photo-electrochemical etching to fabricate single-crystal SiC MEMS for harsh environments. *Materials Letters*, 2011, 65(3): 409-412.
- [42] SHI Y B, SUN Y N, LIU J, et al. UV nanosecond laser machining and characterization for SiC MEMS sensor application. *Sensors and Actuators A: Physical*, 2018, 276: 196-204.

基于波长调制系统的高灵敏度碳化硅 光学 MEMS 加速度计

黄 堃^{1,2}, 程 林², 曲 帅², 刘馥湘², 崔建功², 贺鑫慧², 胡 琴²

(1. 山西师范大学 现代文理学院转设筹备处, 山西 临汾 041000;

2. 中北大学 省部共建动态测试技术国家重点实验室, 山西 太原 030051)

摘要: 本文报道了一种基于双模波长调制的高频碳化硅(Silicon carbide, SiC)传感器及其在并光学微机电系统(Microelectromechanical systems, MEMS)中应用。基于碳化硅材料属性及双模分析,设计了一种适用于高频场的光学 MEMS 传感器,并利用 ANSYS 有限元分析(Finite element analysis, FEA)方法和严格耦合波分析(Rigorous coupled wave analysis, RCWA)方法,将其与其他高频传感器进行性能比较。结果表明,该光学传感器在整个操作测量范围内可提供 $2.2477(\Delta\lambda/\Delta a)$ 的光学灵敏度、 0.155 nm/g 的机械灵敏度和几乎为零的交叉轴灵敏度,且第一谐振频率为 40.035 kHz ,线性测量范围为 $\pm 129.03\text{ g}$,传感系统灵敏度 $(\Delta\lambda/\Delta a)$ 为 0.3484 nm/g ,工作带宽为 35 kHz 。

关键词: 微机电系统; 波长调制; 光学加速度计

引用格式: HUANG Kun, CHENG Lin, QU Shuai, et al. High-sensitivity silicon carbide optical MEMS accelerometer based on wavelength modulation system. Journal of Measurement Science and Instrumentation, 2023, 14(1): 116-126. DOI: 10.3969/j.issn.1674-8042.2023.01.014